Electronic Supplementary Material (ESI) for Metallomics.

Supporting Information

Enhancement of Antipseudomonal Activity of Luminescent Iridium(III) Dipyridylamine Complexes under Visible Blue Light.

Elodie Sauvageot, Margaux Elie, Sylvain Gaillard,* Richard Daniellou, Pierre Fechter, Isabelle J. Schalk,[c] Véronique Gasser, Jean-Luc Renaud* Gaëtan L. A. Mislin*

Table of Content

Part 1: Photophysical properties of complexes (**1**)-(**3**)

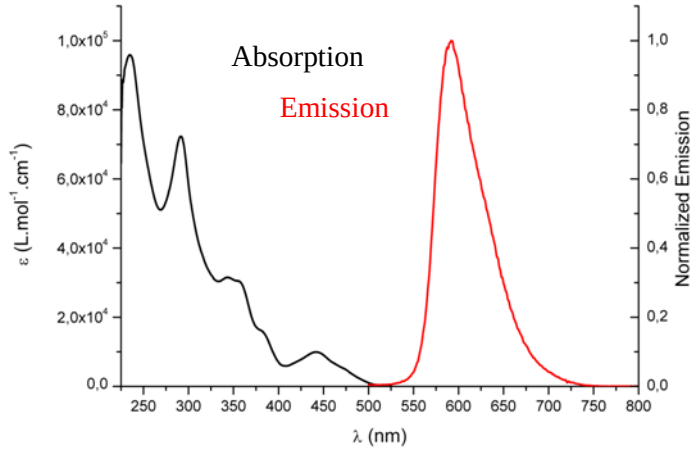

Fig. S1. Absorption and emission spectra of complex (**1**) in CH_2Cl_2.

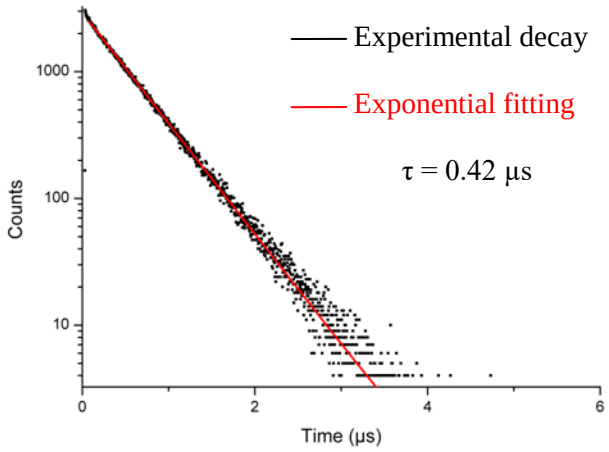

Fig. S2. Excited state lifetime measurement of complex (**1**).

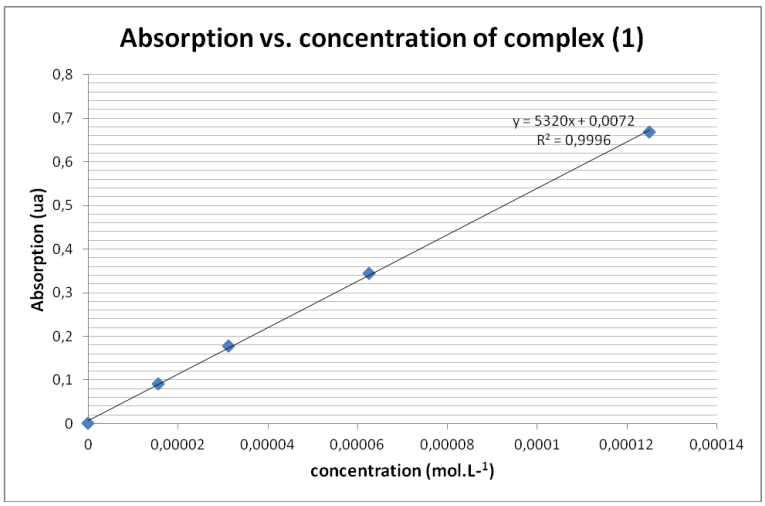

Fig. S3. Linear regression of absorption at 457 nm *vs.* concentration of complex (**1**).

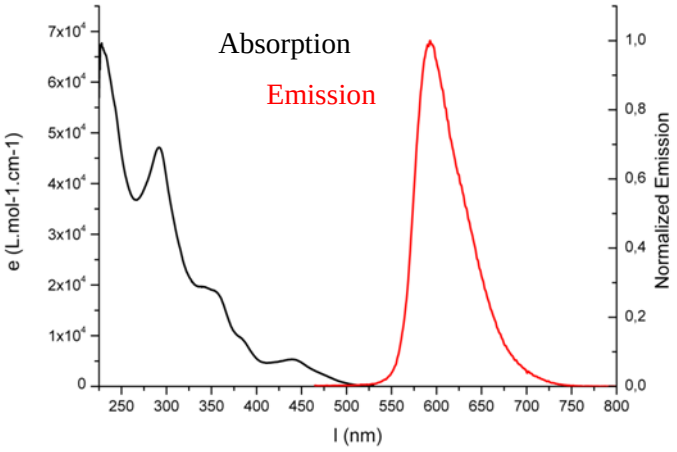

Fig. S4. Absorption and emission spectra of complex (**2**) in CH_2Cl_2.

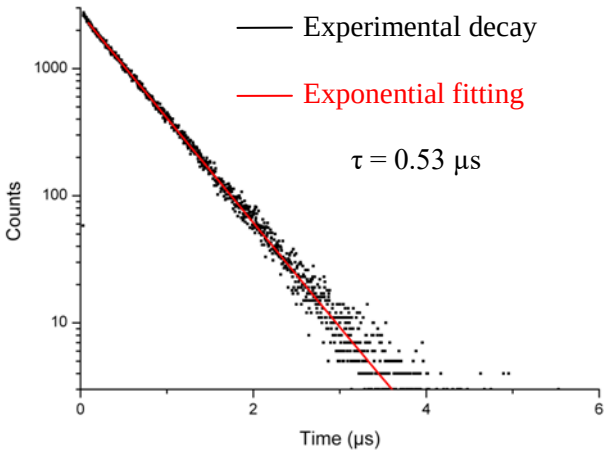

Fig. S5. Excited state lifetime measurement of complex (**2**).

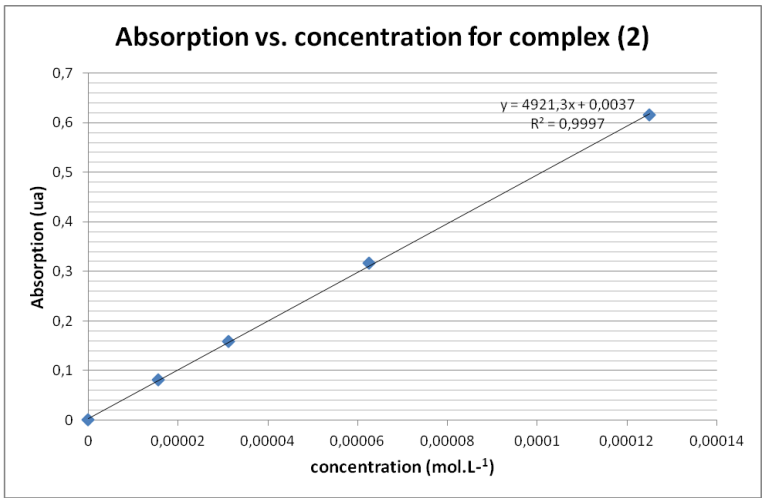

Fig. S6. Linear regression of absorption at 457 nm *vs.* concentration of complex (**2**).

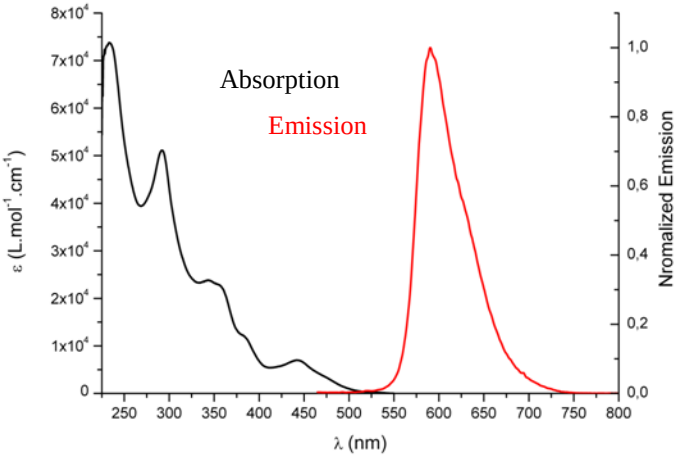

Fig. S7. Absorption and emission spectra of complex (**3**) in CH_2Cl_2.

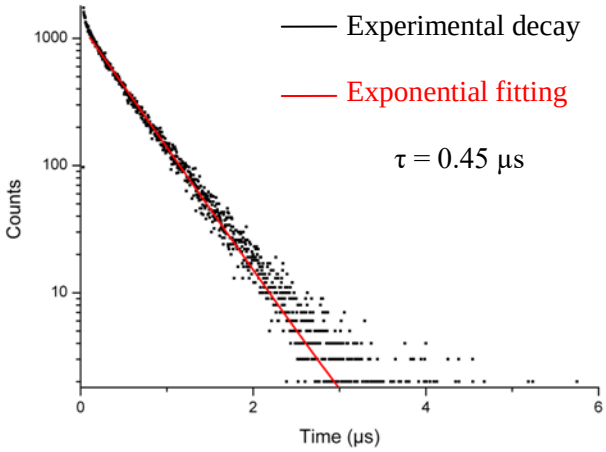

Fig. S8. Excited state lifetime measurement of complex (**3**).

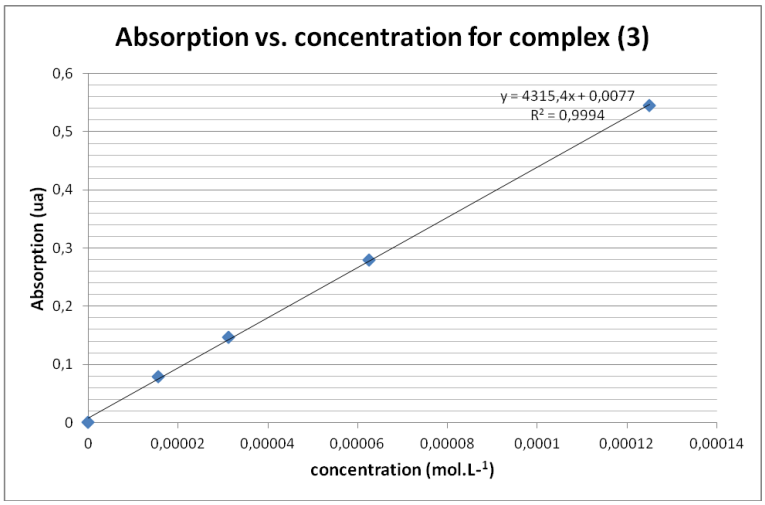

Fig. S9. Linear regression of absorption at 457 nm *vs.* concentration of complex (**3**).

Part 2: ^{1}H and ^{13}C-NMR spectra

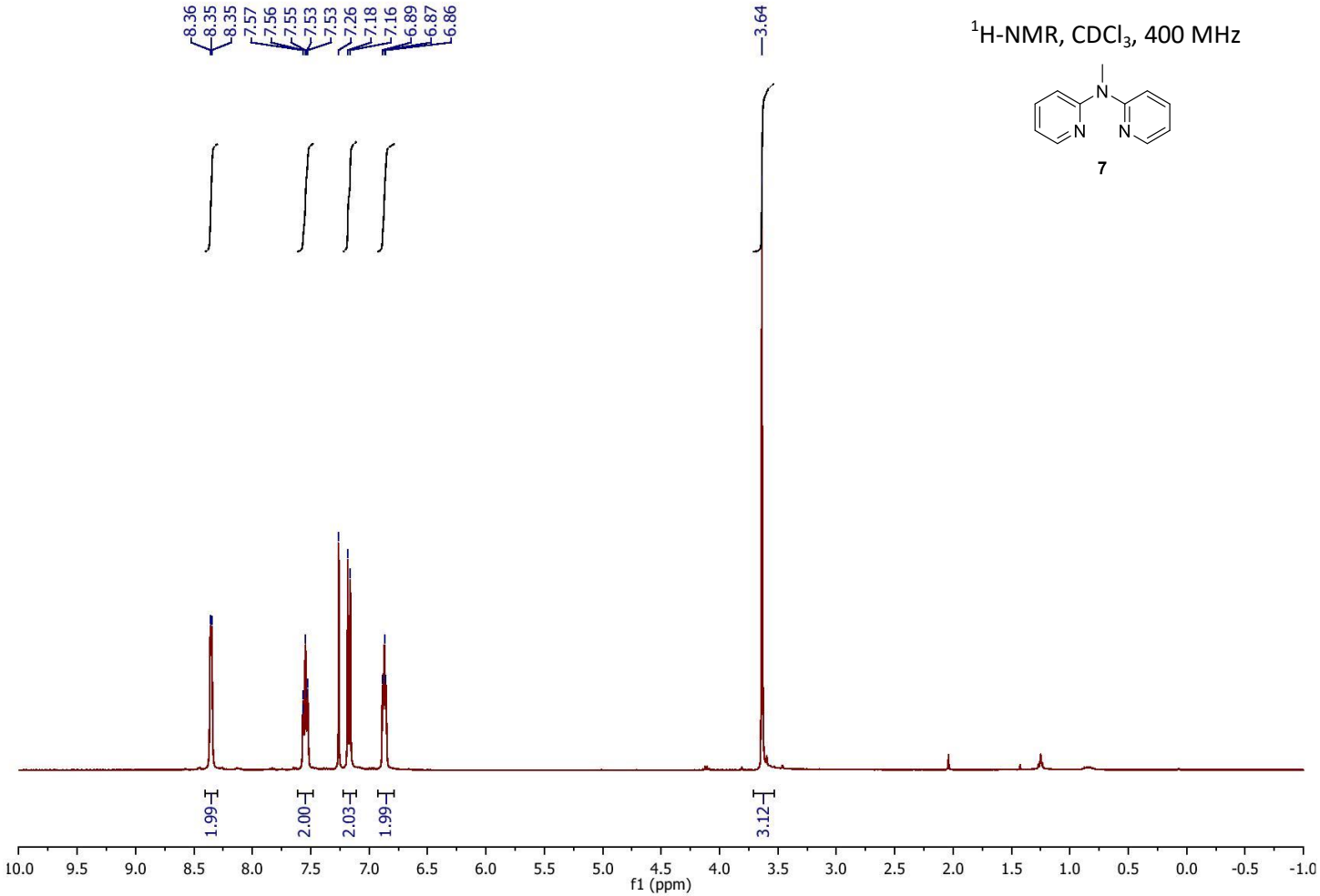

Fig. S10. ^{1}H-NMR spectrum of *N*-(methyl)-*N*-(pyridine-2-yl)pyridine-2-amine (**7**)

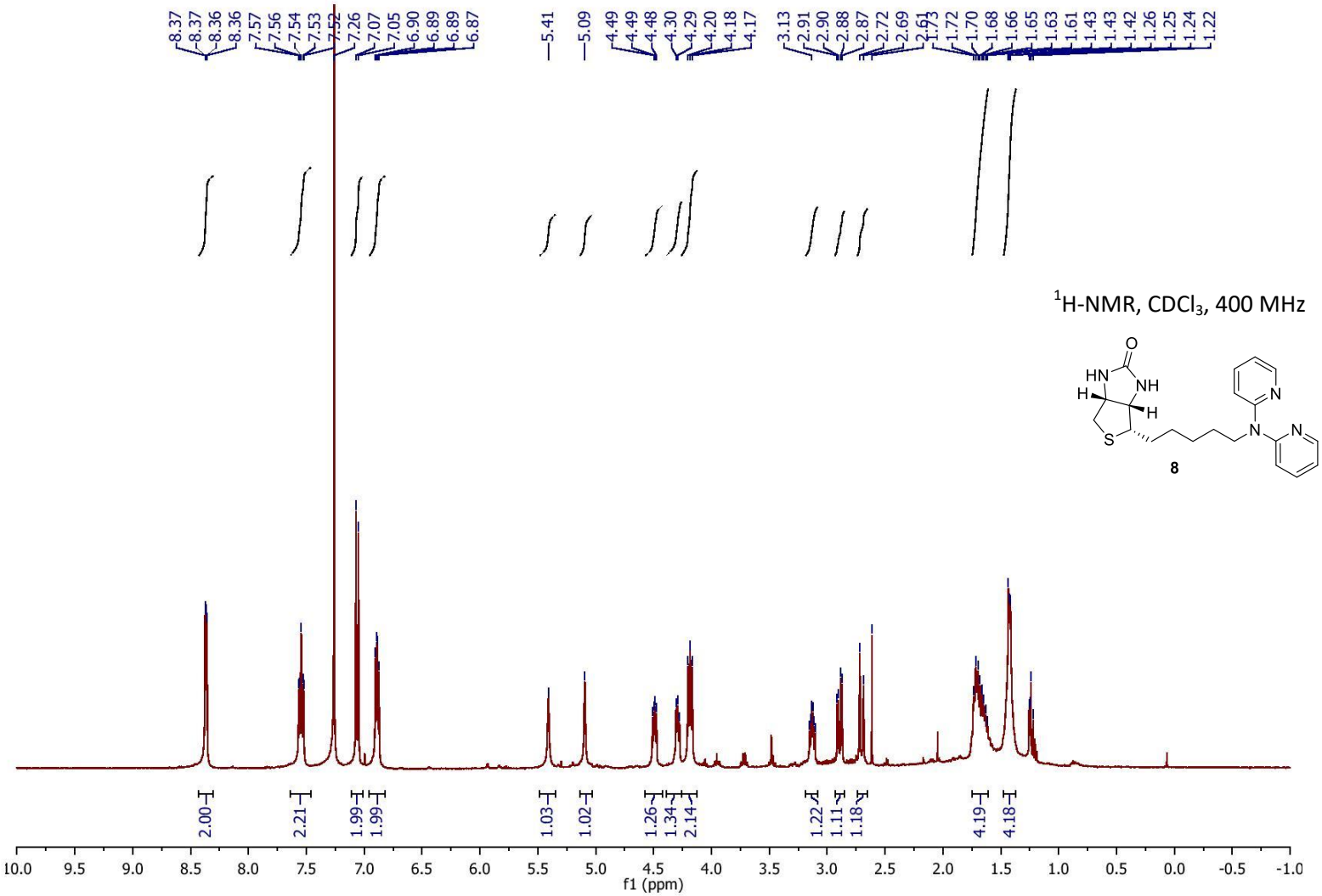

Fig. S11. ^{1}H-NMR spectrum of (3a*S*,4*S*,6a*R*)-4-(5-(di(pyridin-2-yl)amino)pentyl)tetrahydro-1*H*-thieno[3,4-*d*]imidazol-2(3*H*)-one (**8**).

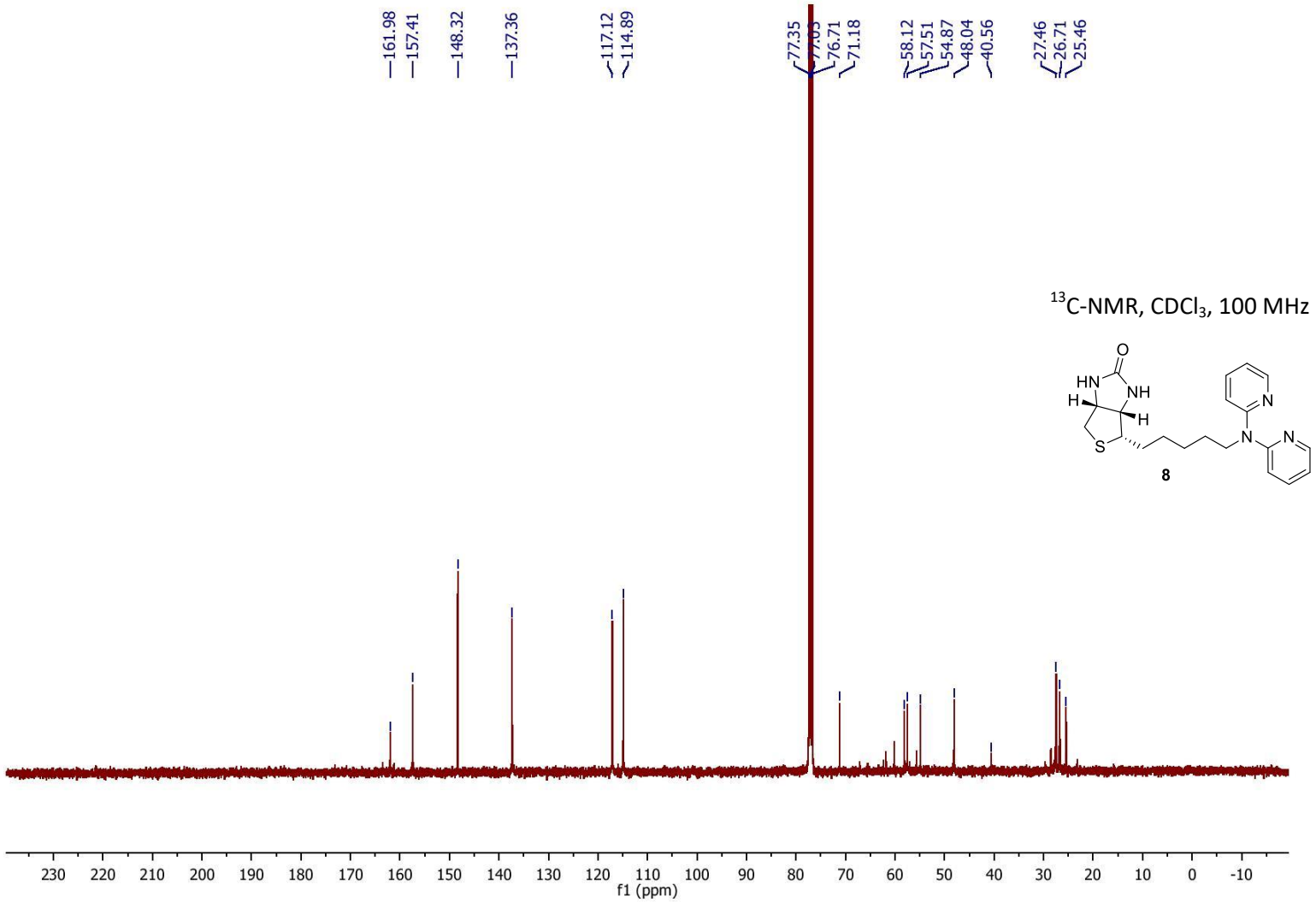

Fig. S12. ^{13}C-NMR spectrum of (3a*S*,4*S*,6a*R*)-4-(5-(di(pyridin-2-yl)amino)pentyl)tetrahydro-1*H*-thieno[3,4-*d*]imidazol-2(3*H*)-one (**8**).

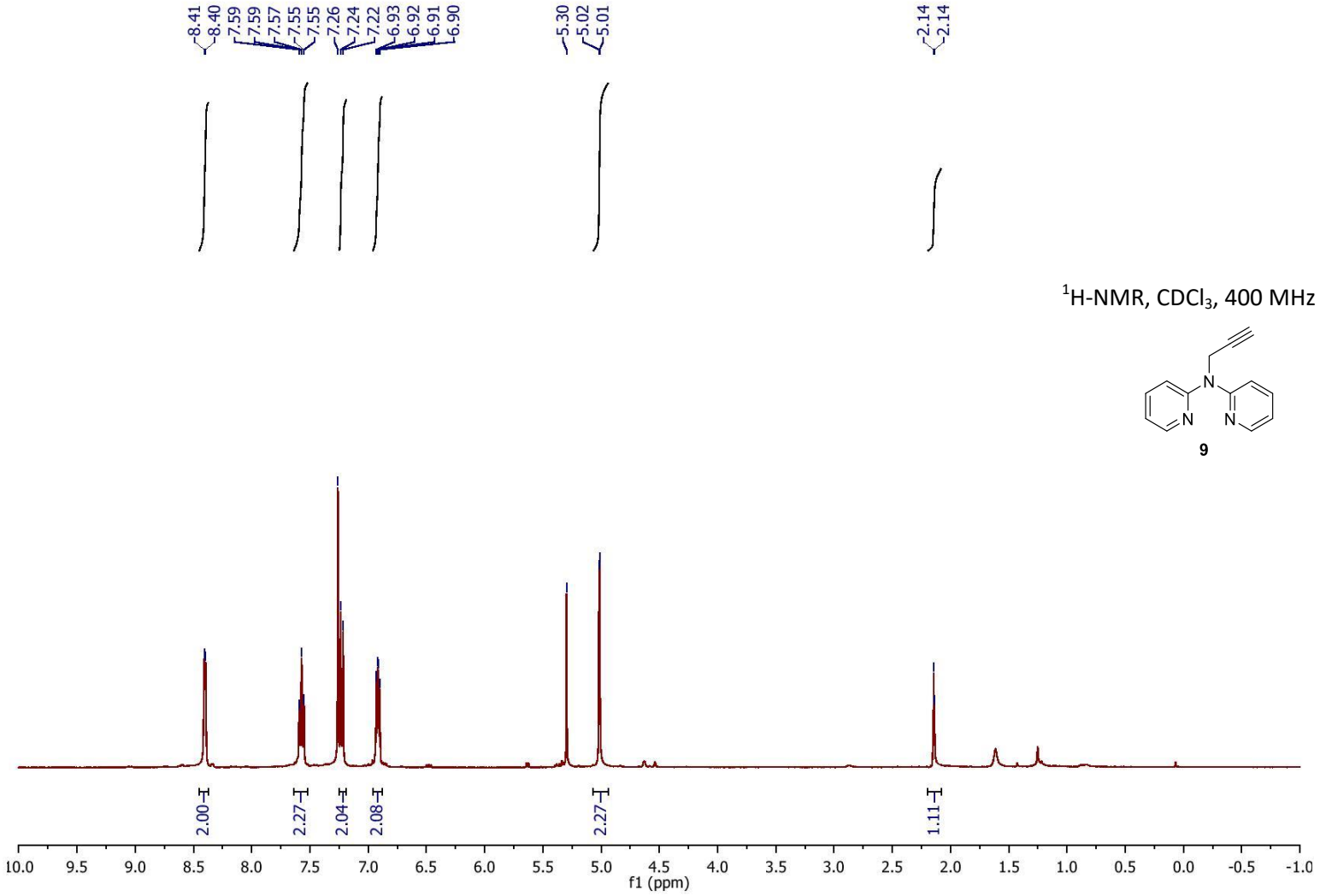

Fig. S13. ^{1}H-NMR spectrum of *N*-(prop-2-yn-1-yl)-*N*-(pyridin-2-yl)pyridin-2-amine (**9**).

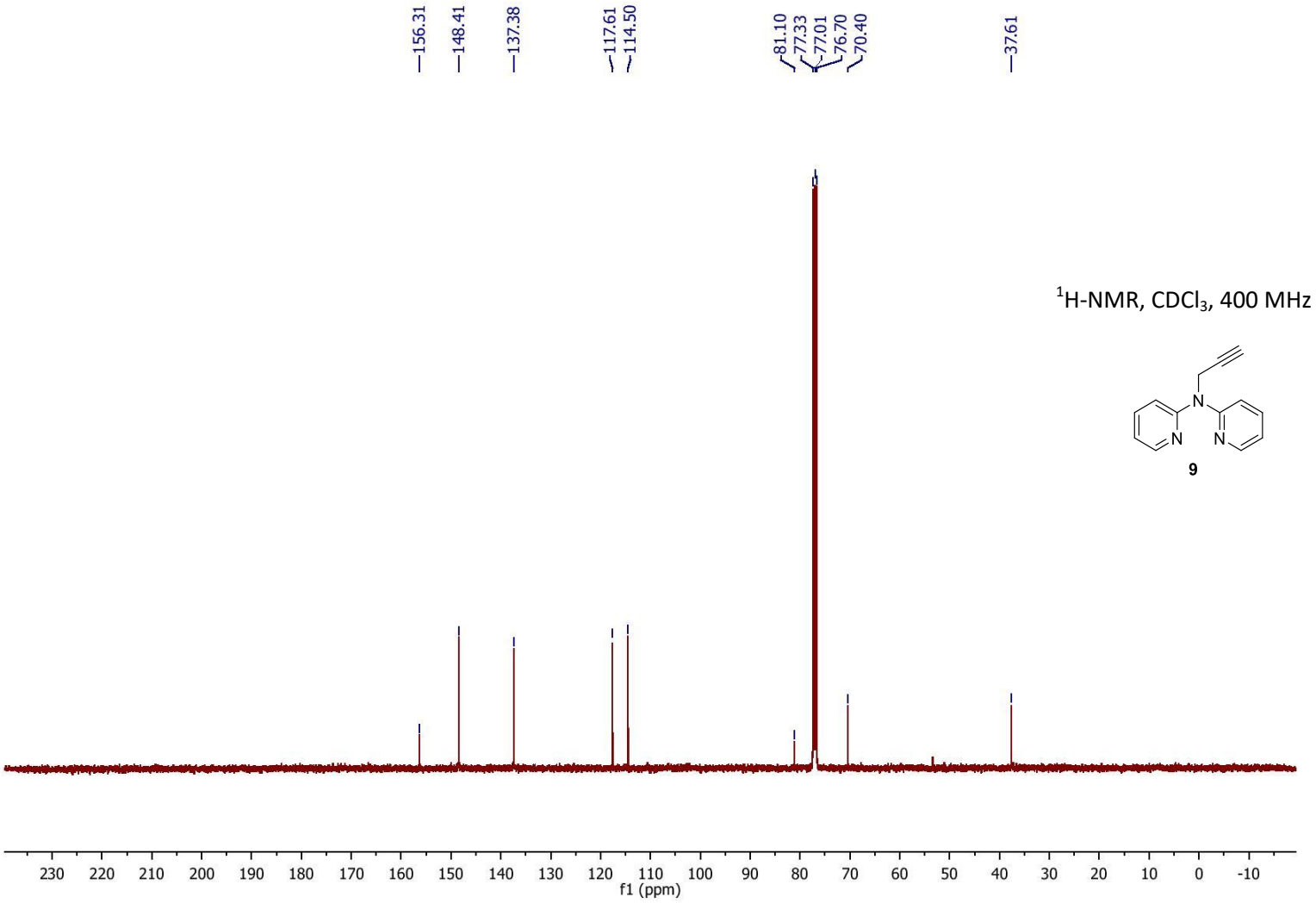

Fig. S14. ^{13}C-NMR spectrum of *N*-(prop-2-yn-1-yl)-*N*-(pyridin-2-yl)pyridin-2-amine (**9**).

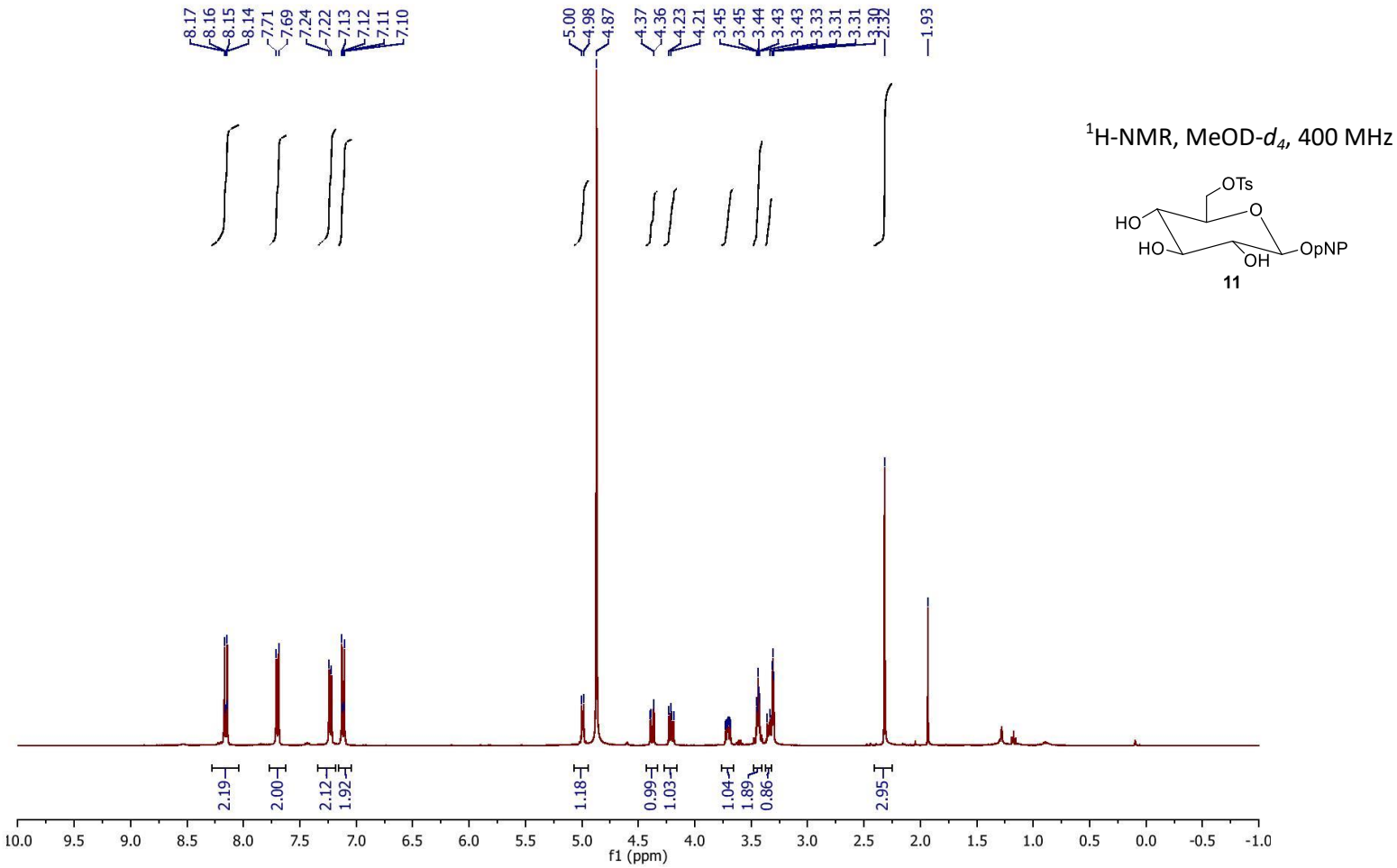

Fig. S15. ^{1}H-NMR spectrum of ((2*R*,3*S*,4*S*,5*R*,6*S*)-3,4,5-trihydroxy-6-(4-nitrophenoxy)tetrahydro-2*H*-pyran-2-yl)methyl-4-methylbenzenesulfonate (**11**).

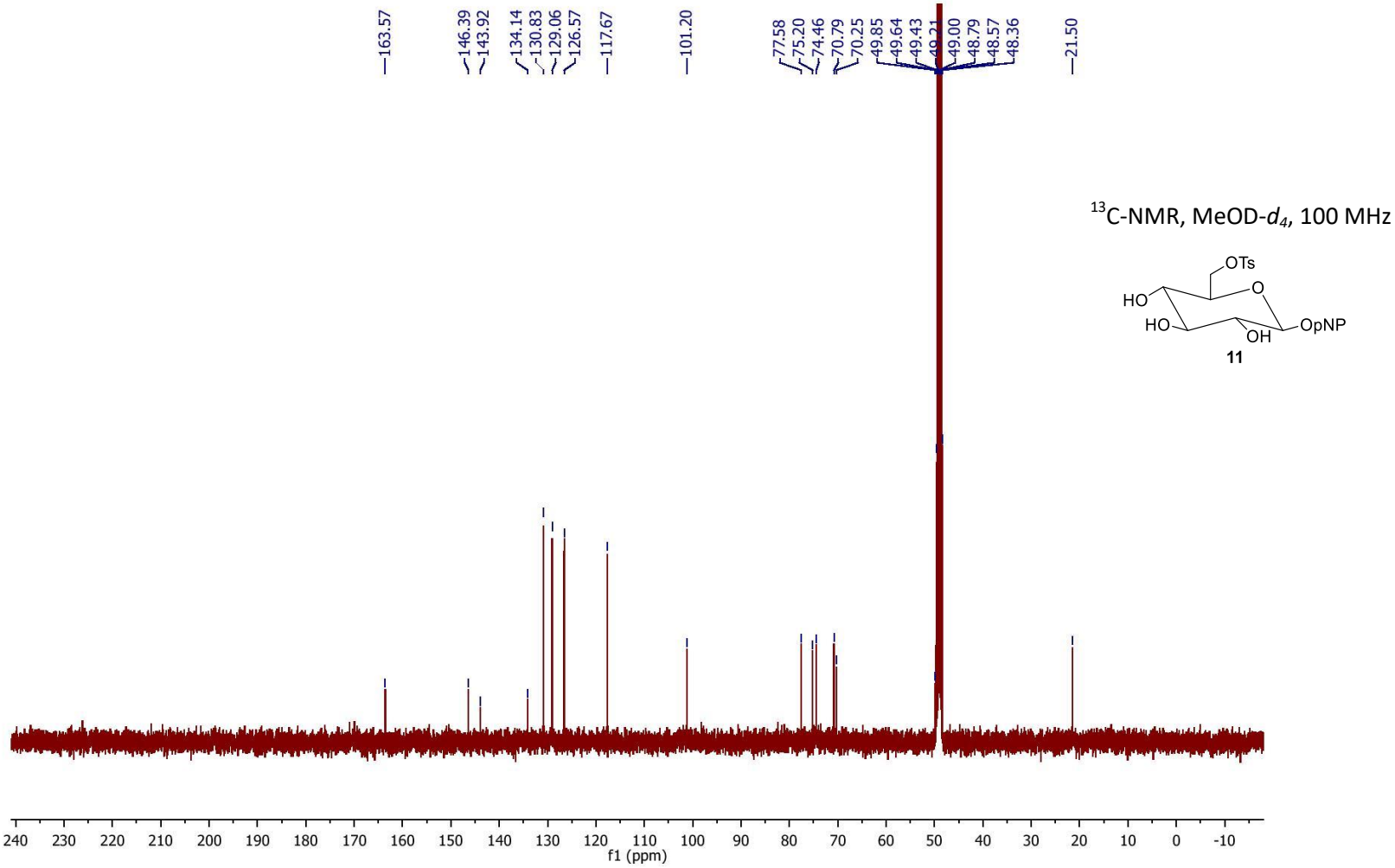

Fig. S16. ^{13}C-NMR spectrum of ((2*R*,3*S*,4*S*,5*R*,6*S*)-3,4,5-trihydroxy-6-(4-nitrophenoxy)tetrahydro-2*H*-pyran-2-yl)methyl-4-methylbenzenesulfonate (**11**)

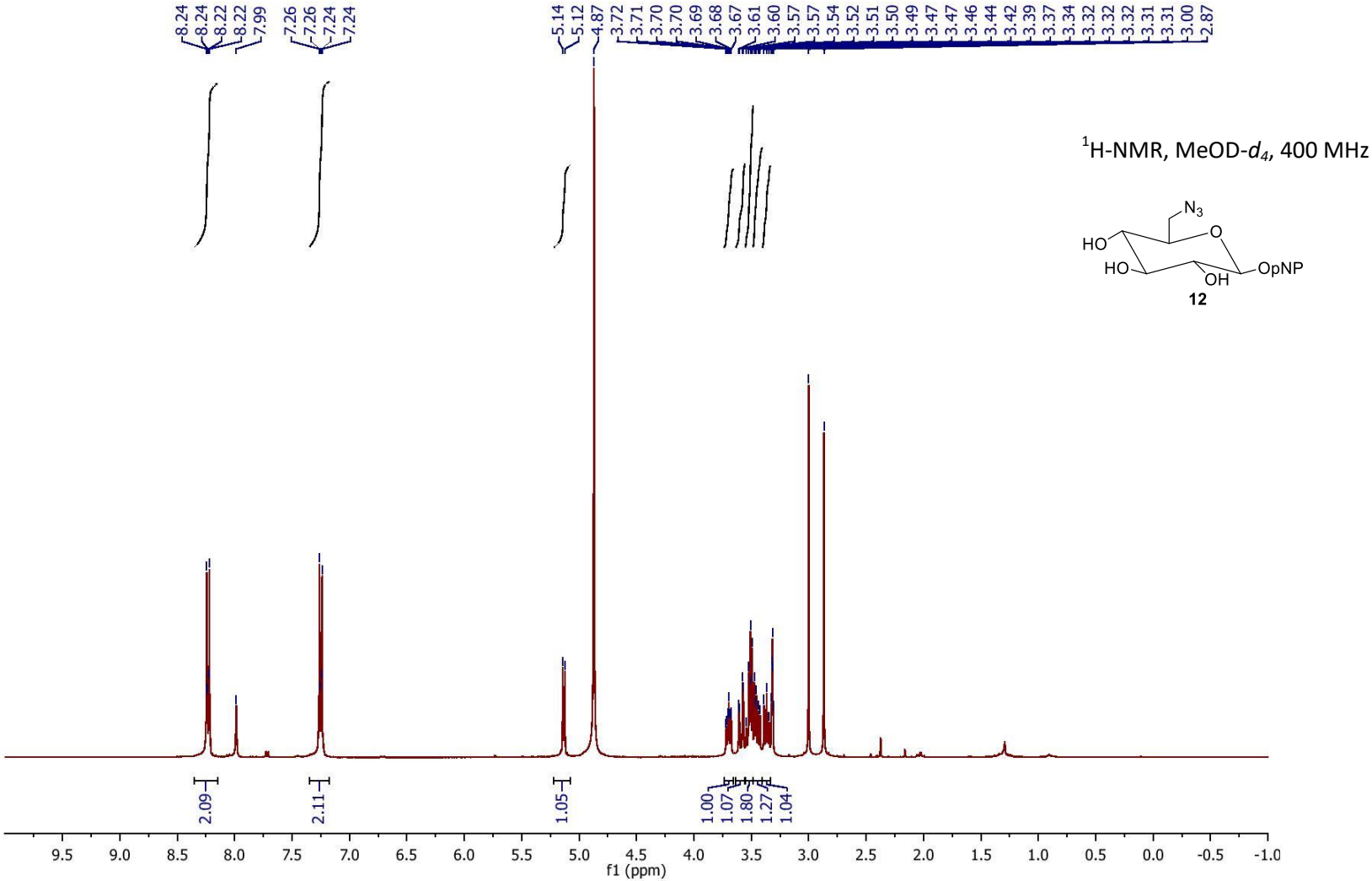

Fig. S17. [1]H-NMR spectrum of (2*R*,3*S*,4*S*,5*R*,6*S*)-2-(azidomethyl)-6-(4-nitrophenoxy)tetrahydro-2*H*-pyran-3,4,5-triol (**12**).

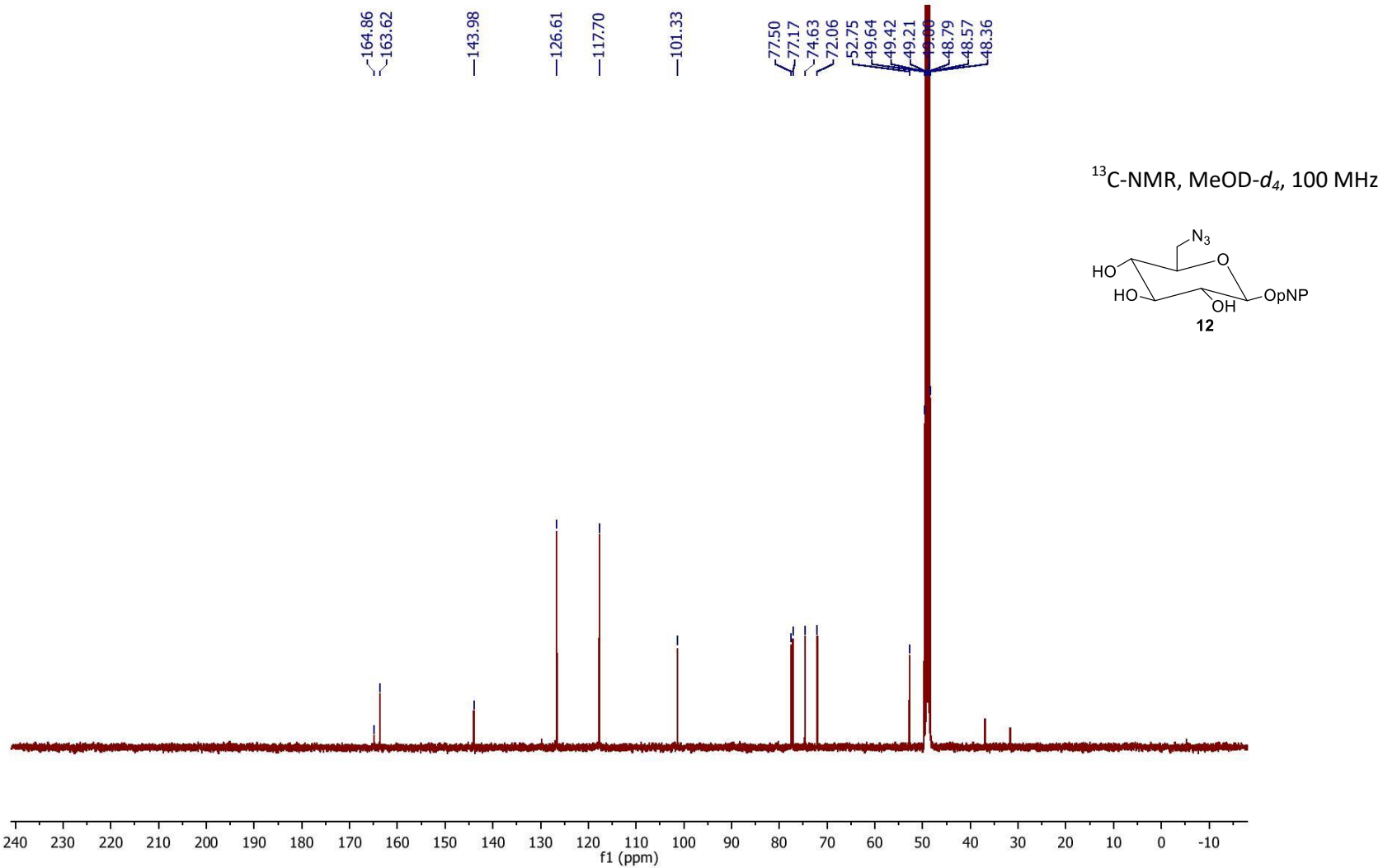

Fig. S18. ^{13}C-NMR spectrum of (2*R*,3*S*,4*S*,5*R*,6*S*)-2-(azidomethyl)-6-(4-nitrophenoxy)tetrahydro-2*H*-pyran-3,4,5-triol (**12**).

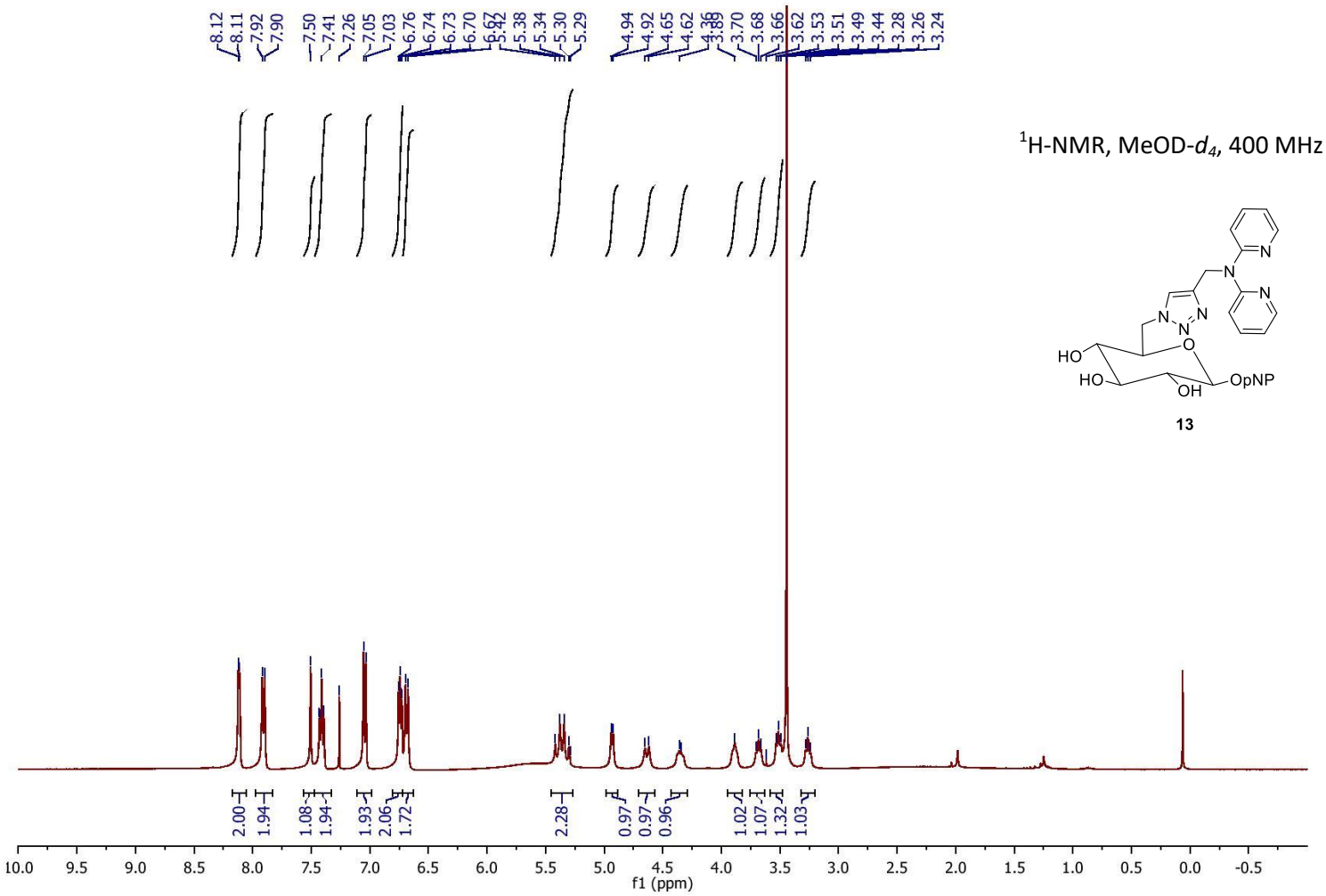

Fig. S19. ^{1}H-NMR spectrum of 2*R*,3*S*,4*S*,5*R*,6*S*)-2-((4-((di(pyridin-2-yl)amino)methyl)-1*H*-1,2,3-triazol-1-yl)methyl)-6-(4-nitrophenoxy)tetrahydro-2*H*-pyran-3,4,5-triol (**13**).

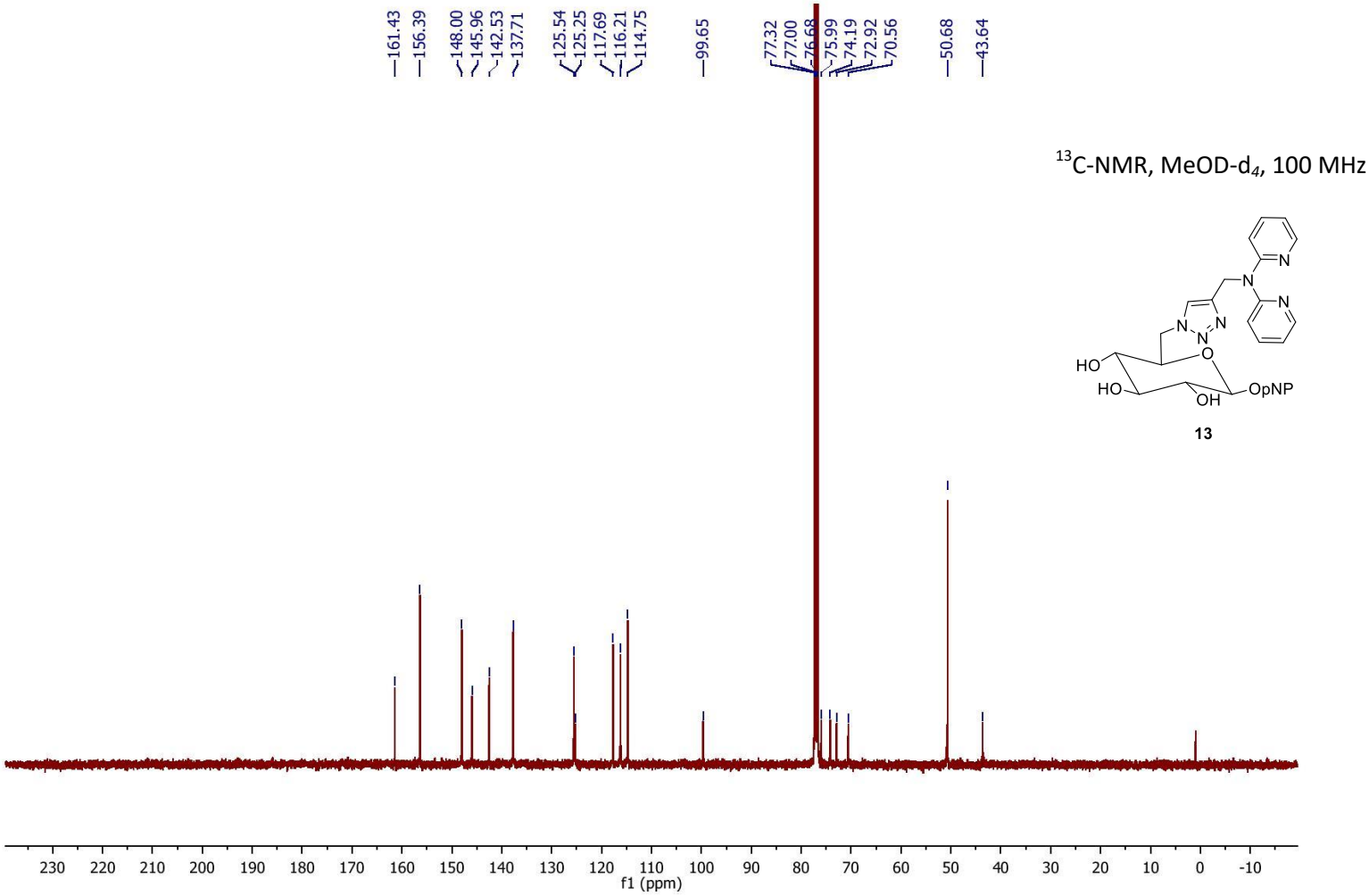

Fig. S20. ^{1}H-NMR spectrum of 2*R*,3*S*,4*S*,5*R*,6*S*)-2-((4-((di(pyridin-2-yl)amino)methyl)-1*H*-1,2,3-triazol-1-yl)methyl)-6-(4-nitrophenoxy)tetrahydro-2*H*-pyran-3,4,5-triol (**13**).

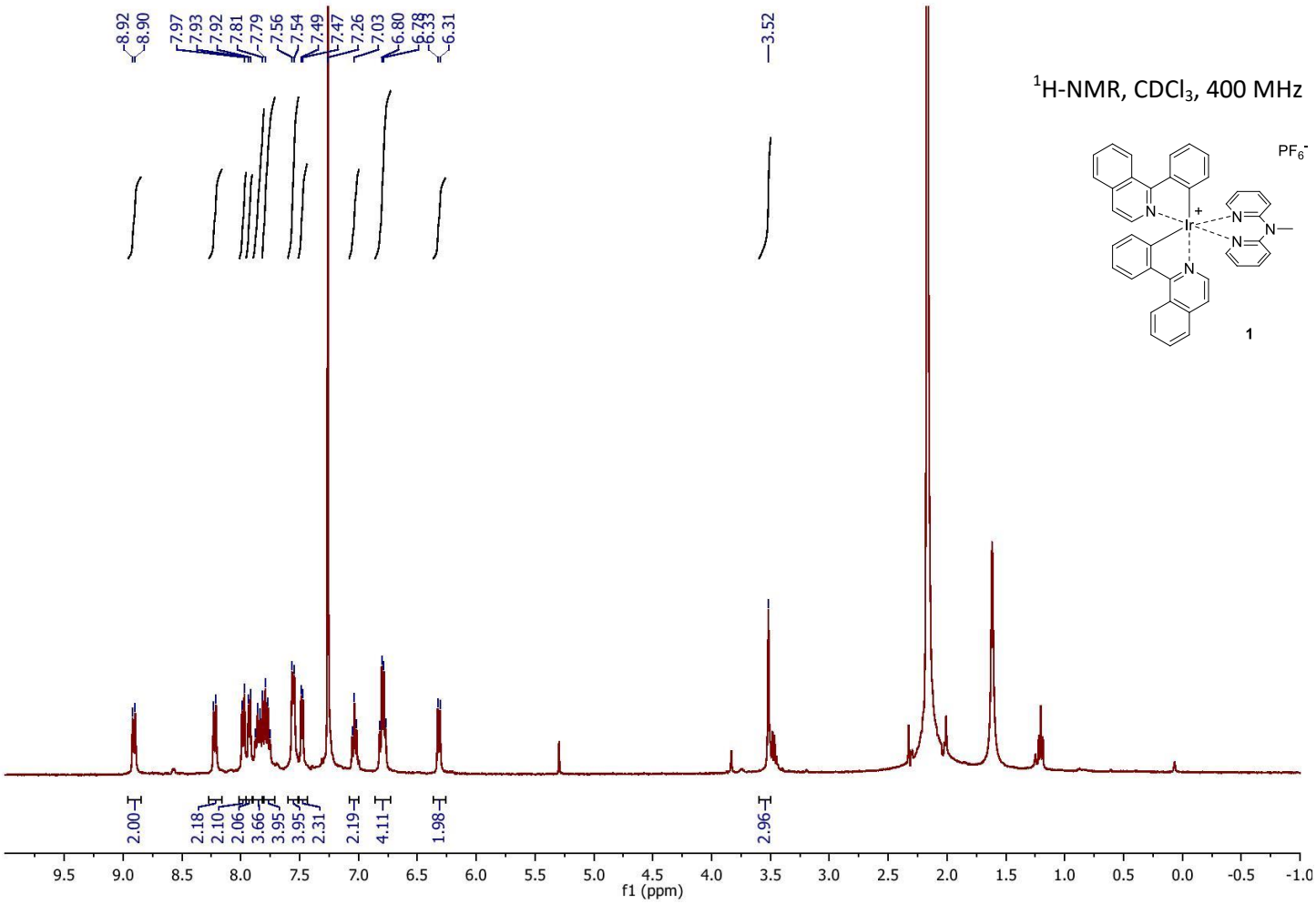

Fig. S21. ^{1}H-NMR spectrum of [(*N*-(methyl)-*N*-(pyridin-2-yl)pyridin-2-amine)bis-(2-phenyl(1-isoquinolinato)-C^2,*N*)iridium(III)] hexafluorophosphate, [Ir(**piq**)$_2$(**7**)][PF_6] (**1**).

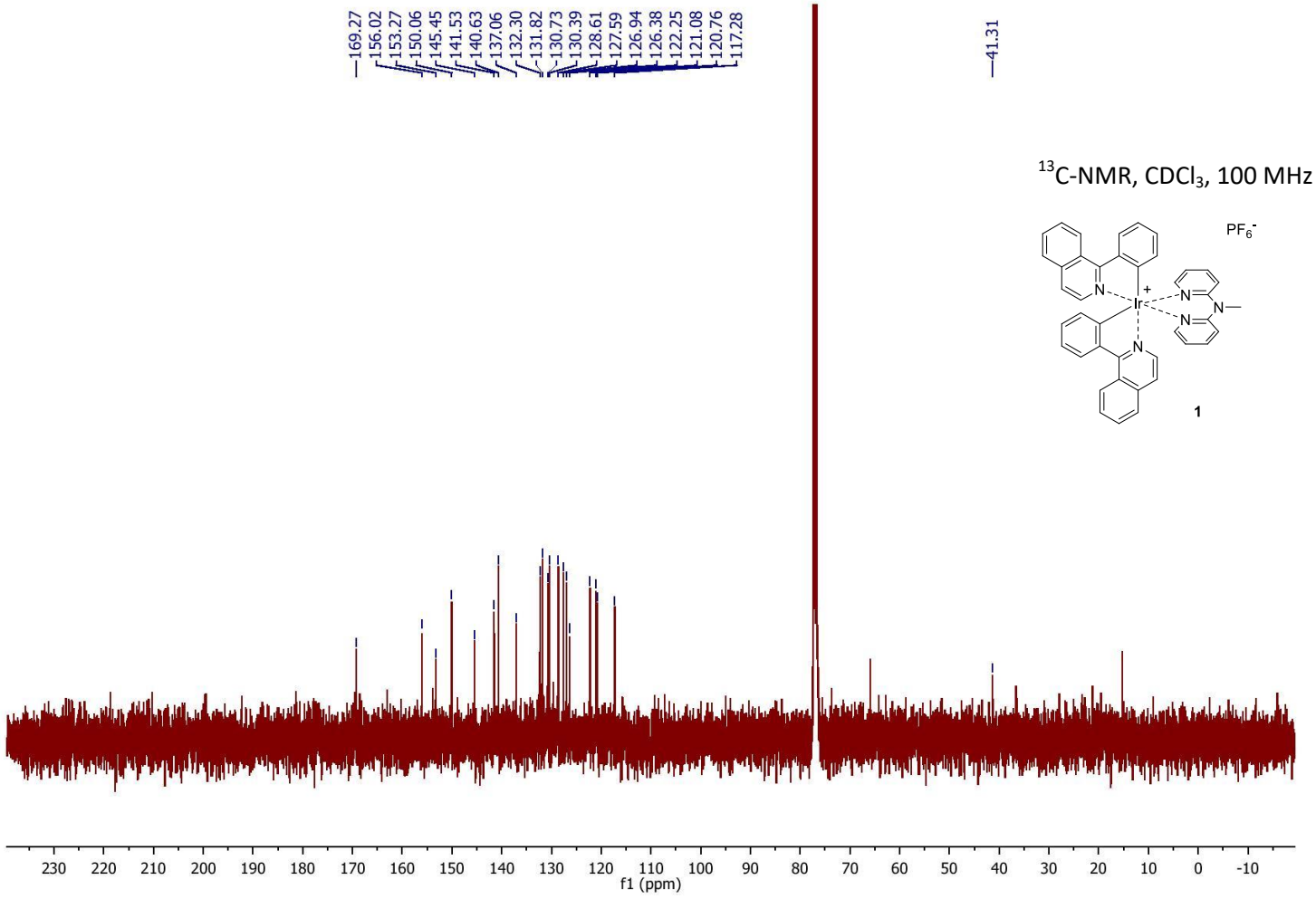

Fig. S22. ^{13}C-NMR spectrum of [(*N*-(methyl)-*N*-(pyridin-2-yl)pyridin-2-amine)bis-(2-phenyl(1-isoquinolinato)-C^2,*N*)iridium(III)] hexafluorophosphate, [Ir(**piq**)$_2$(**7**)][PF_6] (**1**).

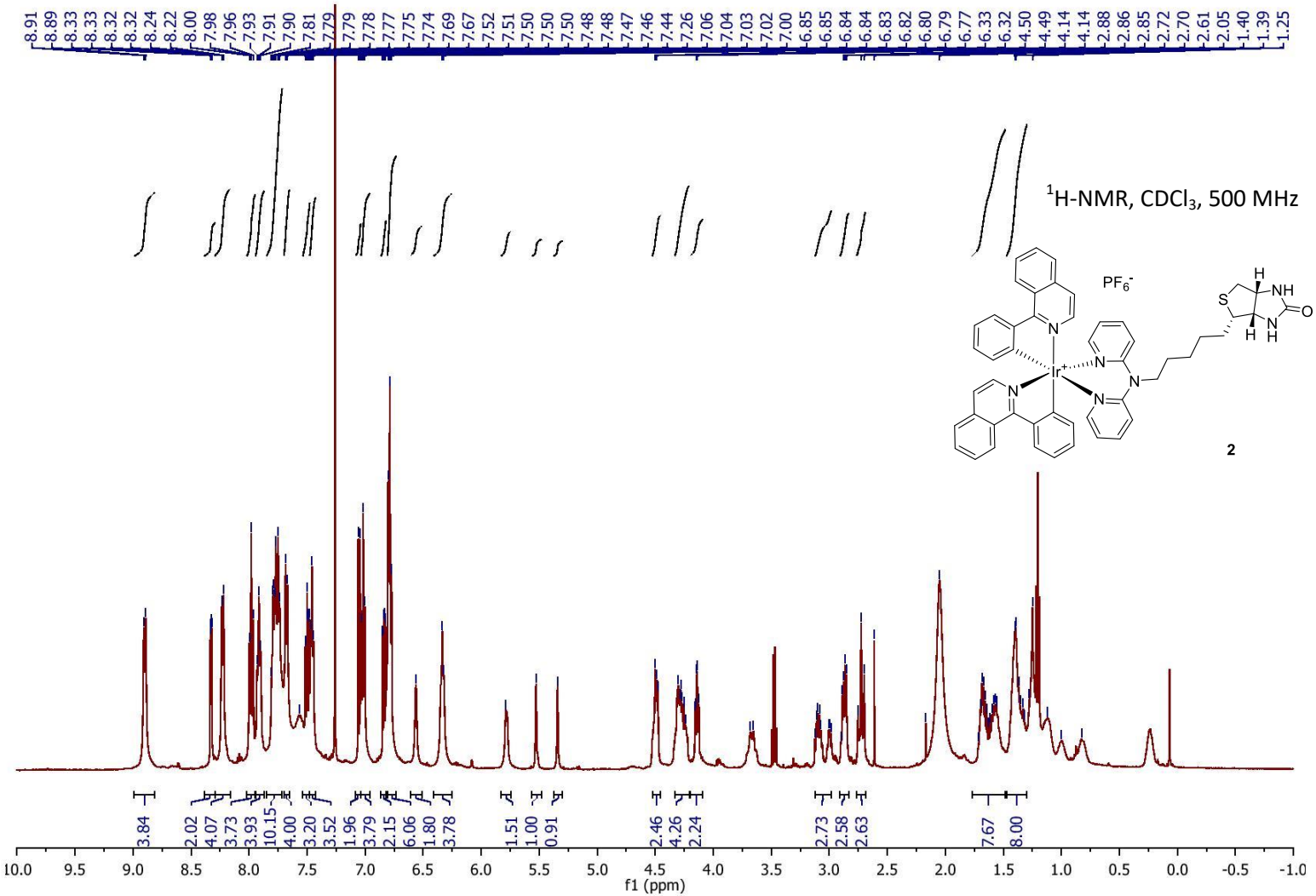

Fig. S23. ^{1}H-NMR spectrum of [Ir(piq)$_2$(**8**)][PF$_6$] (**2**).

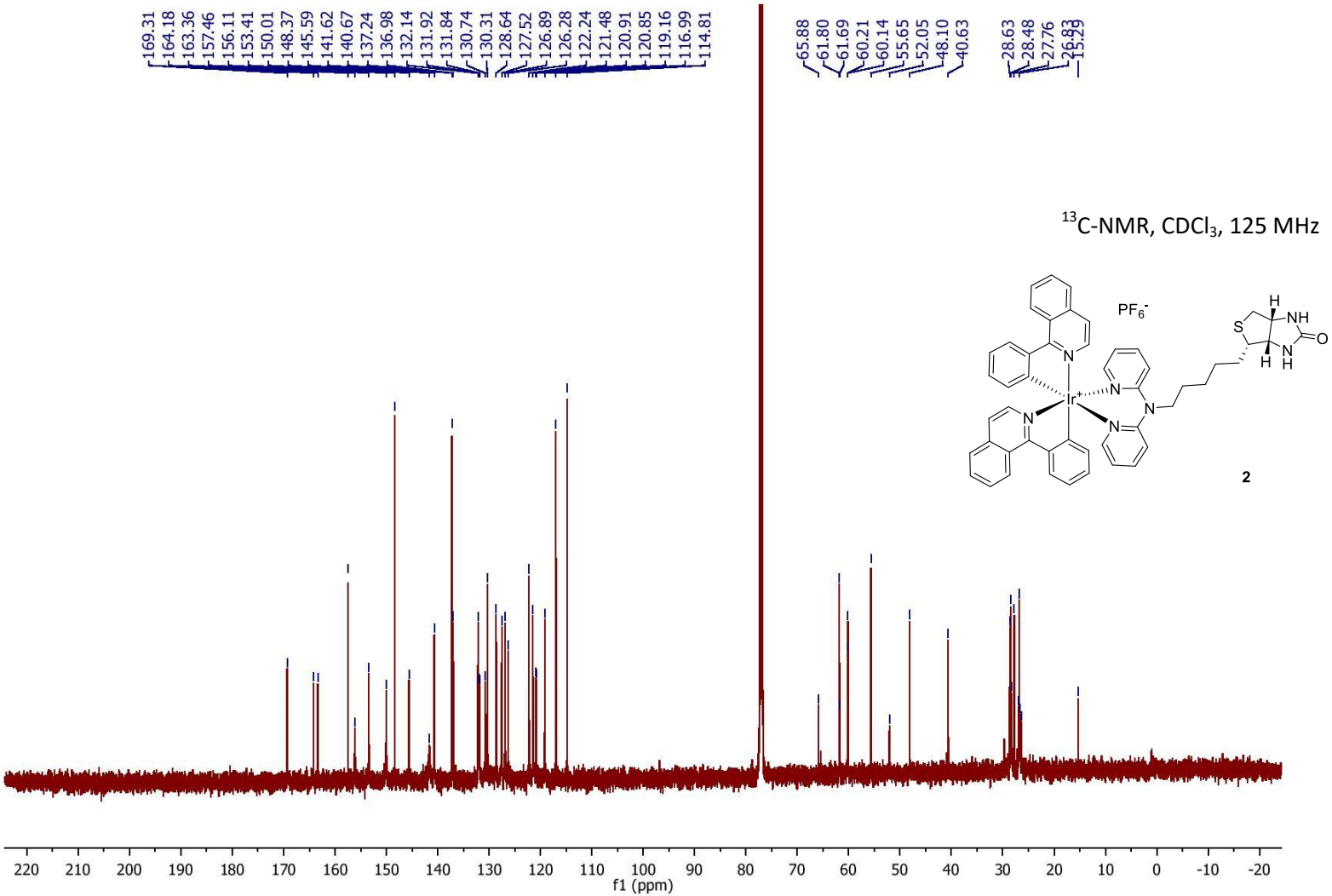

Fig. S24. ^{13}C-NMR spectrum of [Ir(piq)$_2$(**8**)][PF$_6$] (**2**).

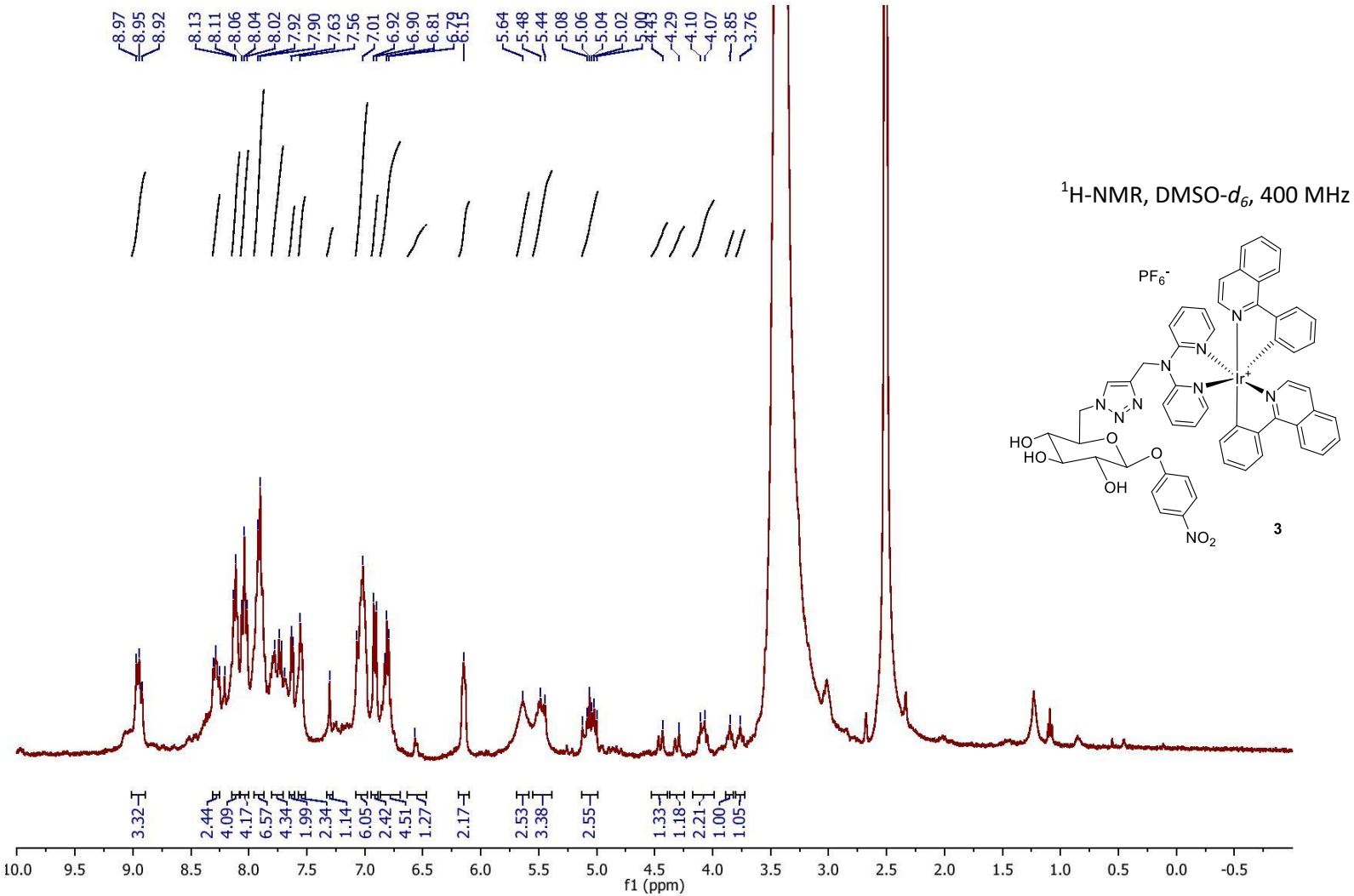

Fig. S25. ^{1}H-NMR spectrum of [Ir(**piq**)$_2$(**13**)][PF_6] (**3**).

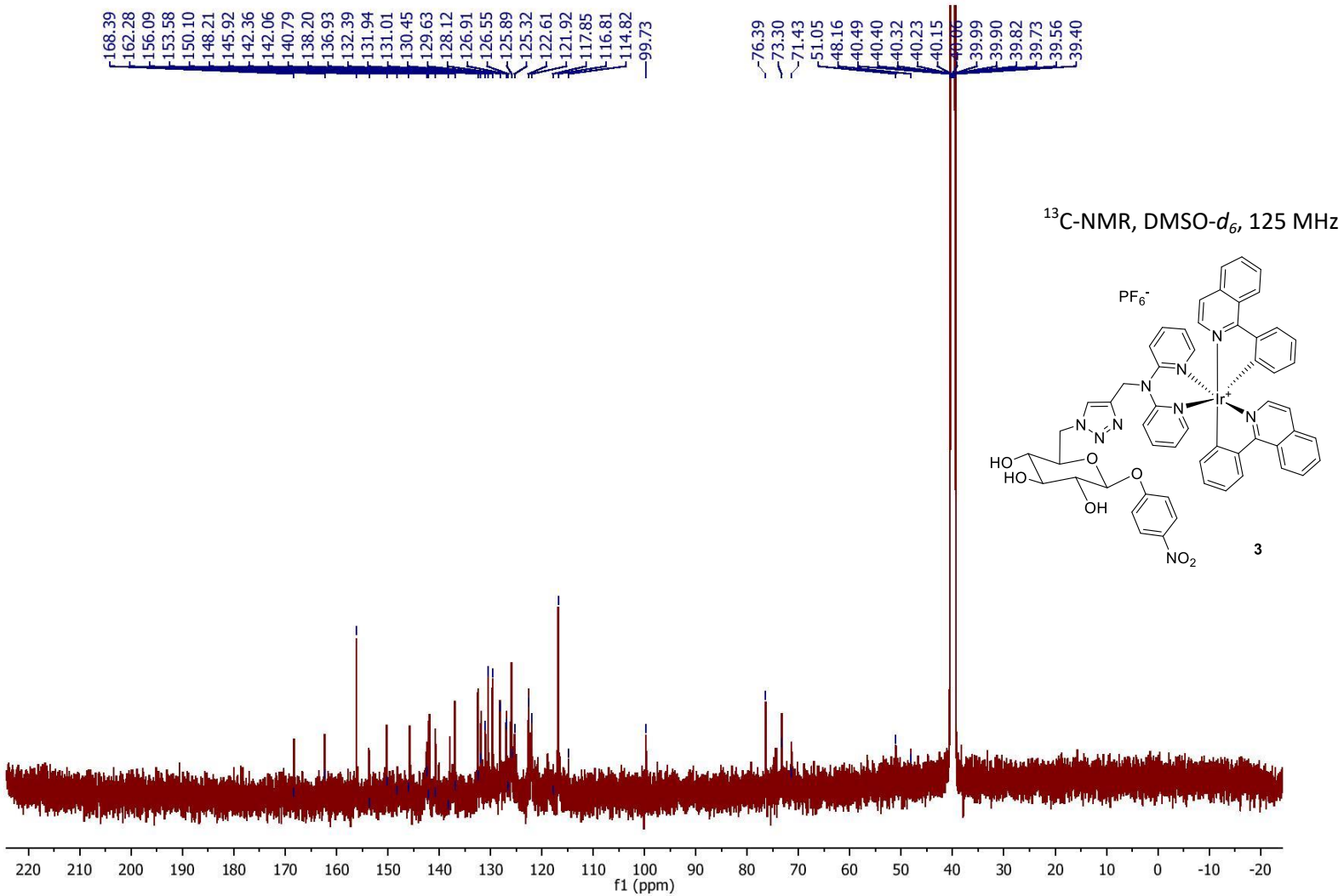

Fig. S26. ^{13}C-NMR spectrum of [Ir(**piq**)$_2$(**13**)][PF_6] (**3**).

Part 3: Pictures and emission spectrum of the photoincubator

Fig. S27. Pictures of the irradiation device. 45 LEDs (3.45 W, 25 Lumen, FlexLED Inspire; www.erp-inspire.com) arranged helicoidally inside a metal cyclinder (h = 22 cm, diam.= 18 cm). A video is available on https://youtu.be/gMmTJuYzAhY.

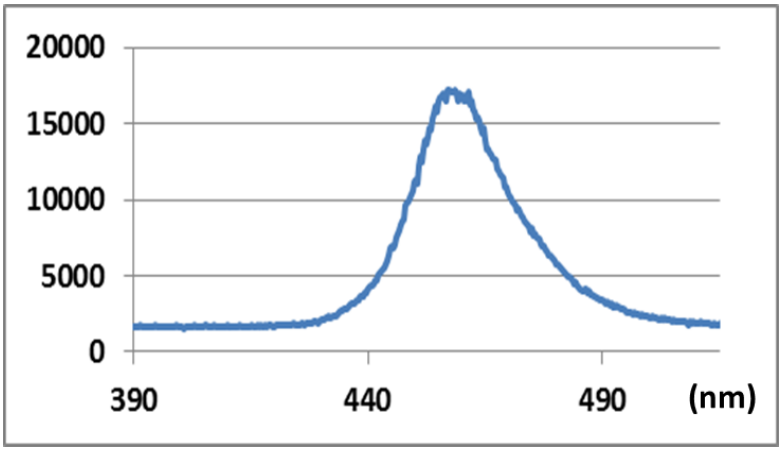

Fig. S28. Emission spectrum of the irradiation device.